

STAR: Shape-focused Texture Agnostic Representations for Improved Object Detection and 6D Pose Estimation

Peter Hönig , Stefan Thalhammer , Jean-Baptiste Weibel ,
Matthias Hirschmanner , and Markus Vincze 

Abstract—Recent advances in machine learning have greatly benefited object detection and 6D pose estimation for robotic grasping. However, textureless and metallic objects still pose a significant challenge due to fewer visual cues and the texture bias of CNNs. To address this issue, we propose a texture-agnostic approach that focuses on learning from CAD models and emphasizes object shape features. To achieve a focus on learning shape features, the textures are randomized during the rendering of the training data. By treating the texture as noise, the need for real-world object instances or their final appearance during training data generation is eliminated. The TLESS and ITODD datasets, specifically created for industrial settings in robotics and featuring textureless and metallic objects, were used for evaluation. Texture agnosticity also increases the robustness against image perturbations such as imaging noise, motion blur, and brightness changes, which are common in robotics applications. Code and datasets are publicly available at github.com/hoenigpeter/randomized_texturing.

I. INTRODUCTION

Object detection and 6D pose estimation are the foundation of robotic grasping [2]. Textured objects are omnipresent in current robotics research since texture cues help modern learned approaches [30]. However, metallic, ceramic, and plastic objects exhibit little to no texture. Furthermore, robot application scenarios present challenges with dynamically changing lighting conditions, resulting in reflections, brightness changes, and other imaging factors [28], [29]. One way to approach these challenges is using methods that learn representations with large amounts of training data to cover a multitude of actual imaging conditions [25], [32], [34]. Real-world images must be manually annotated, which is time-consuming and limits learning novel objects. As a consequence, recent work has focused on using synthetic training images with annotations computed automatically during the rendering process [4], [15], [23].

Training with synthetic data instead of real-world data results in performance loss due to the domain shift described as the Sim2Real gap [18]. Therefore, synthetic dataset generation research aims to improve model generalization [10], [1], [19] by using methods such as domain randomization [33]. Domain randomization samples objects of interest in randomized domains while varying object positions, background textures, material properties, light source positions, and camera viewpoints. So far, little consideration has been paid to the influence

Peter Hönig, Jean-Baptiste Weibel, Matthias Hirschmanner, and Markus Vincze are with the Automation and Control Institute, TU Wien, Austria {hoenig, weibel, vincze}@acin.tuwien.ac.at

Stefan Thalhammer is with the Department of Industrial Engineering, UAS Technikum Vienna, Austria stefan.thalhammer@technikum-wien.at

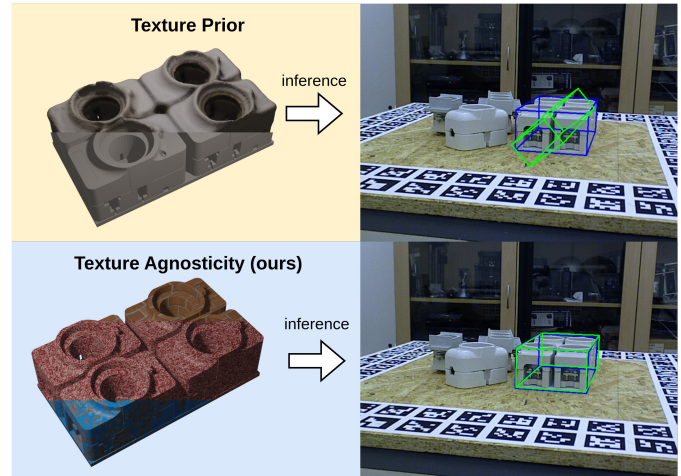


Fig. 1. **Illustration of randomized texturing approach.** 6D pose of object number 8 from the TLESS dataset visualized with 3D bounding boxes; ground truth (blue) and inference (green) using GDR-Net trained with uniform color as prior and with randomized texture.

of the object texture on the encoded representations, although CNNs are prone to learn texture biases. In [8], the authors also show that biasing CNNs toward shape improves ImageNet classification accuracy. We hypothesize that a geometrical bias on shape features is particularly relevant for vision problems with continuous output spaces, such as object detection and pose estimation.

In this work, we present an approach to bias object detectors and pose estimators toward learning shape features using texture-agnostic learning from randomized synthetic data. To generate training data, we randomize object textures repeatedly for each object. The purpose is twofold: a) texture warping on the object surface provides visible features for observing the object geometry in contrast to simply using randomized colors, and b) since encoded representations are agnostic to texture, the trained models generalize to objects with unknown surface texture or color and only object geometries are required as priors. Figure 1 shows an example of training GDR-Net for the TLESS dataset and the influence of randomized texturing on the estimated pose. We evaluate our approach on a variety of object detectors, namely YOLOx [7], Faster R-CNN [26], RetinaNet [21], and 6D pose estimators, namely GDR-Net [34] and Pix2Pose [25]. All models are trained and evaluated with the TLESS [17] and ITODD [5] datasets, which reflect critical robotic challenges, low texture, metallic objects, and occlusion [12], [35]. Our experiments show that for the majority of these cases, the focus on shape features improves the results

compared to using texture priors and that online augmentation hyperparameter tuning leads to state-of-the-art results in the remaining cases.

We summarize our contributions as the following:

- Biasing object detectors and pose estimators toward texture agnosticity makes it possible to rely solely on object geometry as a prior, thereby focusing on object shape rather than texture.
- We show that texture agnosticity increases the robustness w.r.t image perturbations like imaging noise, motion blur, and brightness changes prevalent in robotic applications.
- The correlation between randomized texturing and online data augmentation provides a reference for the balanced integration of both domain randomization methods combined and can be used to improve the performance of detectors or pose estimators in general.
- We conduct experiments on two challenging standard datasets, demonstrating improvements for two recent pose estimation approaches and three standard object detectors. In cases where texture agnosticity is inferior to texture priors, careful online data augmentation hyperparameter tuning still improves estimation accuracy.

The paper is structured as follows: In Section II, we provide an overview of the current state of the art. Section III introduces our shape focusing approach using texture randomization and briefly describes the evaluation process. Traversing to Section V, we present our main results and ablation studies. Section VI concludes by summarizing observations and discussing future work.

II. RELATED WORK

This section summarizes the state of the art for object detection, pose estimation, and data representation.

A. 2D Object Detection and 6D Pose Estimation

Throughout this paper, the term object detection defines the 2D detection of an object, defined by the class label c and bounding box \mathbf{b} . Pose estimation refers to the instance-level 6D pose estimation of an object, defined by the translation \mathbf{T} and rotation \mathbf{R} .

To review the latest advancements in the object detection and pose estimation field, the BOP challenge [14], [16] serves as a significant reference. The BOP challenge ranks the best-performing object detection and pose estimation methods, evaluated with standardized metrics and datasets. Successful object detectors from the last years' challenges include two-stage models such as Mask-RCNN [11] and Faster-RCNN, and single-stage ones, e.g. YOLOx. Besides their use for object searching, object tracking, or visual servoing, these models also provide multi-stage pose estimators with pre-computed regions of interest (ROI). Pose estimators are either composed of a single stage [32], [31] or multiple stages [25], [34], where subsequent stages build upon the ROI provided by an arbitrary object detector. For each ROI, the subsequent steps perform feature extraction, learn 2D-3D correspondences, and regress translation and rotation of the object pose. Successful CNN-based methods [34], [25] from the last years' challenges use multi-stage approaches employing one of the abovementioned

object detectors. For pose estimation, the best-performing models from BOP 2022 predict intermediate representations, such as dense 2D-3D correspondences maps [34], [25] with subsequent Perspective-n-Point (PnP) matching, either via RANSAC or learning-based, for regression of object translation and rotation.

B. Data Representation

The BOP challenge ranks the top-performing object detection and pose estimation methods and features a set of baseline datasets to ensure comparability of the submitted algorithms. Among those datasets are Linemod-Occcluded [13], TLESS [17], ITODD [5], and YCB-V [3], all of which are composed of physically-based-rendered (PBR) training sets and real-world test sets. Popular toolkits to render such datasets are BlenderProc [4], a Python library using the Blender API or UnrealRox [23], which leverages the Unreal Engine as a backbone for rendering.

In order to bridge the domain gap between the simulation and the real-world domain, modern rendering pipelines apply domain randomization [33], including, e.g., the variation of backgrounds, camera views, object poses, and lighting. Depending on the target domain, meshes for the datasets are either provided via CAD modeling or reconstructions [24], [36]. TLESS and ITODD, for example, feature plastic and metallic objects for industrial purposes, where CAD models are usually available. These CAD models are geometrically accurate but often lack texture information. Reconstructed objects are also provided, adding texture information but removing the benefit of the CAD models' high geometrical accuracy because of added reconstruction noise.

After studying the current field of synthetic data generation and domain generalization for object detection and pose estimation, we identify a possible research gap, namely the randomization of object textures, to force CNNs to learn exclusively from object geometries from 2D RGB images only.

III. TEXTURE AGNOSTICITY

This section introduces our novel synthetic training data generation approach, illustrated in Figure 2. Standard approaches assume the object texture given as prior through reconstructing the object or by applying color heuristics for rendering, referred to as texture prior. Instead of relying on the abovementioned strategies, we propose to employ strategies that generate estimators agnostic to object texture, referred to as texture agnosticity. We motivate the texture agnosticity concept by two aspects:

- 1) **Improving automation.** In order to ensure short cycle times of industrial processes, it is preferable to generate training data exclusively from CAD. On the one hand, estimators can already be trained before physical object instances exist. On the other hand, geometrical inaccuracies of the CAD models used for rendering training data are negligible compared to reconstructing physical object instances.
- 2) **Improving estimation.** In [8], the authors show that inducing a shape bias to image classifiers improves classification accuracy. We hypothesize that this trait might

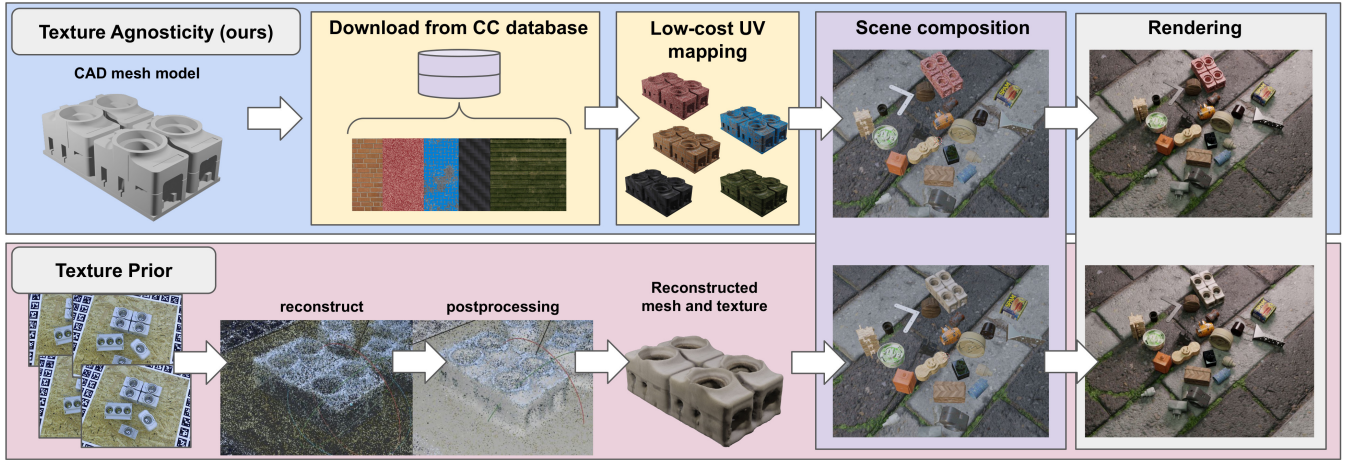


Fig. 2. **Synthetic data generation with randomized texturing pipeline.** We bypass the time-consuming steps of texture modeling or reconstruction using CAD meshes with randomized textures. We retrieve textures from a creative commons texture database and apply them to the CAD mesh model. This path is computationally less expensive compared to the mesh reconstruction procedure, which not only requires the real object and images covering the full object surface, but also a mesh reconstruction step, postprocessing and cropping. This conventional approach is computationally expensive and delivers meshes with reduced quality compared to the CAD model.

be especially beneficial for tasks such as object detection and pose estimation, where learning geometrical features is of primary relevance.

In [8], the authors perform image style transfer with AdaIN [6] to improve the performance of image classification tasks. Despite improving classification accuracy on ImageNet [27], using style transfer approaches is not applicable for generating training data for more complex tasks, e.g., object detection and pose estimation. Applying random styles to scene-level images shifts object borders and leads to ambiguities where objects interact. Since style transfer methods such as [6] do not guarantee geometrically accurate object representations, we propose using a different strategy. We propose to wrap random textures geometrically accurately around objects during the scene composition step of synthetic data generation. During rendering, object borders and mutual object interactions are accurately captured, and as such, the generated training data is well suited for training methods that require accurate object geometries. The proposed approach for inducing texture agnosticity is easily integrable into standard rendering pipelines [4], [23], [15]. Thus, it is applicable and beneficial for various object detection and pose estimation approaches.

A. Inducing Texture Agnosticity

We base our approach on the seminal work of domain randomization from [33]. The authors consider various scene composition parameters, including background texture and camera, object, and light source poses as random variables. Object textures are randomized by assigning a randomly sampled uniform color. In [4], the authors show that randomly sampling textures with repeating patterns as scene backgrounds results in rich backgrounds, suitable for effective foreground-background separation for various vision problems. We hypothesize that applying this strategy for generating object textures results in learning feature spaces that encode the object geometry, similar to [8]. In contrast to assigning a

random uniform color as texture, the proposed strategy allows direct observation of the object geometry based on texture distortion.

B. Training Data Distribution

Let $T = \{T_1, T_2, \dots, T_m\}$ be a set of textures with repeating patterns and $M = \{M_1, M_2, \dots, M_k\}$ a set of objects of interest. The training dataset for M is generated according to the number of scenes $N = \{N_1, N_2, \dots, N_j\}$ and the rendered views per scene. Let n be a hyperparameter, denoting the number of textures of T used for generating N . For each sampled scene O , the texture is drawn based on a uniform distribution $\mathcal{U}_{1,n}$ over T_n , for each sampled object of M . For every scene in S , images I are rendered with randomized object and camera poses, specular and roughness values, and camera-to-object distances.

IV. EXPERIMENTAL SETUP

We evaluate our approach on TLESS and ITODD. These datasets are chosen since they cover textureless and metallic objects, which are highly relevant for industrial automation. TLESS provides reconstructed, as well as color- and textureless meshes, consequently allowing us to ablate the influence of the mesh origin. Concerning object symmetries, we assume that symmetries are fully observable through the object geometry. For dataset rendering, the Blenderproc PBR pipeline [4] is used. Figure 3 illustrates exemplary images, comparing TLESS and ITODD rendered using texture priors and texture agnosticity. We render $I = 50,000$ training images of $O = 2000$ scenes for each of both datasets, which is the standard configuration for BOP. Textures are retrieved from a Creative Commons online texture database (cc-textures)¹. The number of random textures is $n = 1226$ if not stated otherwise. As test sets, we use the ones provided by BOP.

Table I shows the list of parameters and their ranges used for scene composition. For texture agnosticity, we assign specular

¹Public domain textures used: <https://cc0-textures.com/>

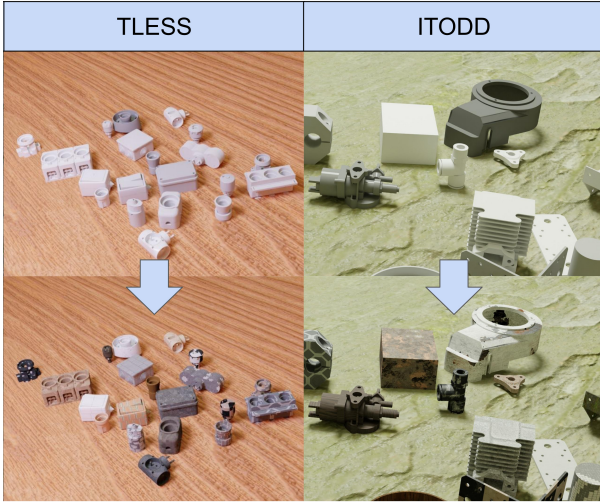


Fig. 3. **Exemplary renderings.** Object textures before and after the randomized texturing approach is applied to the TLESS and ITODD datasets

and roughness values identical to the pipelines for CAD meshes and reconstructed meshes, as implemented in the BOP rendering scripts². The random texture is drawn from T_n .

TABLE I
DOMAIN RANDOMIZATION OVERVIEW. PARAMETERS AND FUNCTIONS DENOTING THE RENDERING SPECIFICATIONS FOR THE TLESS AND ITODD OBJECTS

Method	Parameter	Function
Texture prior	Specularity	$S \sim \mathcal{U}(0, 1)$
	Roughness	$R \sim \mathcal{U}(0, 1)$
	Color	$(R, G, B) \sim \mathcal{U}(0.1, 0.9)$
Texture agnosticity	Specularity	$S \sim \mathcal{U}(0, 1)$
	Roughness	$R \sim \mathcal{U}(0, 1)$
	Color	$(R, G, B) = T_{n \sim \mathcal{U}(1, 1226)}$

A. Evaluation Metrics

We provide the COCO evaluation metric [20] for object detection, namely the mean average precision mAP at an intersection over union (IoU) of 0.5 : 0.95. N denotes the number of categories, while AP_i^t is the average precision for category i at a specific IoU threshold t .

$$mAP = \frac{1}{N} \sum_{i=1}^N \frac{1}{9} \sum_{t=0.5}^{0.95} AP_i^t \quad (1)$$

For pose estimation, we report the average recalls of visible surface discrepancy (VSD) [14], maximum symmetry-aware surface distance (MSSD) [5], and maximum symmetry-aware projection distance (MSPD) [16].

$$VSD = \text{avg}_{p \in V_{UV}} \begin{cases} 0 & \text{if } p \in \hat{V} \cap \bar{V} \wedge |\hat{D}(p) - \bar{D}(p)| < \tau \\ 1 & \text{otherwise} \end{cases} \quad (2)$$

²https://github.com/DLR-RM/BlenderProc/tree/main/examples/datasets/bop_challenge

$$MSSD = \min_{S \in S_M} \max_{\mathbf{x} \in V_M} \|\hat{\mathbf{P}}\mathbf{x} - \bar{\mathbf{P}}\mathbf{S}\mathbf{x}\|_2 \quad (3)$$

$$MSPD = \min_{S \in S_M} \max_{\mathbf{x} \in V_M} \|\text{proj}(\hat{\mathbf{P}}\mathbf{x}) - \text{proj}(\bar{\mathbf{P}}\mathbf{S}\mathbf{x})\|_2 \quad (4)$$

Visible Surface Discrepancy (VSD): VSD calculates the pixel-wise difference between the estimated $\hat{D}(p)$ and ground truth $\bar{D}(p)$ distance map for pixels p visible in the estimated \hat{V} and ground truth \bar{V} image. τ acts as a misalignment tolerance. Since VSD is only calculated over visible pixels, it is a suitable metric for robotic manipulation, where only visible and, therefore, graspable surfaces matter.

Maximum Symmetry-Aware Surface Distance (MSSD): MSSD calculates the distance between points on the object’s surface after symmetry transformations S are applied to vertices $\mathbf{x} \in V_M$ of a model M , given the estimated \hat{P} and ground truth \bar{P} poses. Similar to VSD, the MSSD metric is well-suited for evaluating pose estimation performance regarding robotic grasping, which measures how significantly the surfaces of estimated and ground truth objects differ without accounting for occlusion.

Maximum Symmetry-Aware Projection Distance (MSPD): MSPD calculates the distance between points on the object’s surface projected to 2D. Similar to MSSD, 3D surface points are calculated by applying symmetry transformations S to vertices $\mathbf{x} \in V_M$ for a model M , given the estimated \hat{P} and ground truth \bar{P} poses. By focusing on 2D projections, MSPD is particularly well-suited for RGB-only methods, where estimation along the optical Z-axis is challenging.

A combined recall from VSD, MSSD, and MSPD is provided with the overall recall score $AR = (AR_{VSD} + AR_{MSSD} + AR_{MSPD})/3$. For pose estimation ablations, we also report the average recall of ADD(-S), which is the average distance of model points m , for $k_m d \geq m$, with the error threshold k_m set to 10% [13]. Let \mathbf{x} denote a model point from mesh M . $\hat{\mathbf{R}}$ and $\hat{\mathbf{T}}$ denote the estimated rotation and translation, whereas $\bar{\mathbf{R}}$ and $\bar{\mathbf{T}}$ denote the ground truth.

$$m = \text{avg}_{\mathbf{x} \in M} \begin{cases} \left\| (\bar{\mathbf{R}}\mathbf{x} + \bar{\mathbf{T}}) - (\hat{\mathbf{R}}\mathbf{x} + \hat{\mathbf{T}}) \right\| & \text{unsym.} \\ \min_{\mathbf{x}_2 \in M} \left\| (\bar{\mathbf{R}}\mathbf{x} + \bar{\mathbf{T}}) - (\hat{\mathbf{R}}\mathbf{x}_2 + \hat{\mathbf{T}}) \right\| & \text{sym.} \end{cases} \quad (5)$$

B. Online Data Augmentation

To establish the relation of texture agnosticity to online data augmentation, we define specific sets of augmentation based on the problem. Table II presents the augmentations and ranges used for object detection and pose estimation. These ranges are used across all models if not mentioned otherwise. We introduce the coefficient λ , with $p_{ablation} = \lambda p$, for varying the intensity of the applied data augmentations. Data augmentation for object detection is used as introduced in the YOLOx version, winning the 2022 BOP object detection challenge of BOP [22], [30]. The online data augmentation of GDR-Net [34] is used for pose estimation.

TABLE II

DATA AUGMENTATION. BASELINES FOR OBJECT DETECTION AND POSE ESTIMATION; p DENOTES AUGMENTATION PROBABILITY

Object Detection		Pose Estimation	
Augmentation	p	Augmentation	p
Coarse Dropout	0.5	Coarse Dropout	0.5
Gaussian Blur	0.4	Gaussian Blur	0.5
Enhance Sharpness	0.3	Add	0.5
Enhance Contrast	0.3	Invert	0.3
Enhance Brightness	0.5	Multiply	0.5
Enhance Color	0.3	Linear Contrast	0.5
Add	0.5		
Invert	0.3		
Multiply	0.5		
Additive Gaussian Noise	0.1		
Linear Contrast	0.5		

V. EMPIRICAL EVALUATION OF TEXTURE AGNOSTICITY

This section presents experimental results for object detection and pose estimation accuracy improvement when using our proposed randomized texturing approach. The experiments also provide information on the relationship between randomized texturing and online data augmentation. Ultimately, we demonstrate that inducing a geometry bias during pose estimator training increases the robustness against image perturbations during runtime. This improved robustness is particularly valuable for robotic applications, where factors such as imaging noise, motion blur, and changing brightness must be considered.

A. Main Results

The following paragraphs quantify object detection and pose estimation accuracy improvements when inducing texture agnosticity through randomized texturing.

1) *Detection Accuracy*: Table III shows the mAP results using texture priors and texture agnosticity for YOLOx, Faster R-CNN, and RetinaNet trained on TLESS and ITODD. The models are trained under two conditions, with ($\lambda = 1$) and without ($\lambda = 0$) online data augmentations.

For TLESS, the randomized texturing variants of YOLOx, Faster R-CNN, and RetinaNet consistently outperform the baseline methods trained without affine online color space data augmentations, just using the standard geometric augmentations, as is the case for the methods [26] and [21]. Performance differences up to 36.75% are observed, indicating a significant improvement. The behavior is similar for ITODD. When online data augmentations are applied, a slight decrease in performance of up to 6.51% is noted on TLESS compared to the baseline results. In the case of ITODD, all detectors show increased performance when texture agnosticity is combined with online data augmentation. Figure 4 shows example images of the ITODD dataset with bounding boxes predicted by YOLOx using texture priors and texture agnosticity. The baseline model of YOLOx shows a false positive detection on the background and significantly inaccurate bounding box corners on the actual object. In contrast, the randomized texturing version results in a true positive detection with accurately regressed bounding box corners.

TABLE III

OBJECT DETECTION. $\text{MAP}^{0.50:0.95}$ SCORES FOR YOLOx [7], FASTER R-CNN [26], AND RETINANET [21] TRAINED ON TLESS AND ITODD WITH ORIGINAL (ORIG.) AND RANDOMIZED TEXTURES (OURS)

Dataset		no Aug. $\lambda = 0$			with Aug. $\lambda = 1$		
		[7]	[26]	[21]	[7]	[26]	[21]
TLESS	Orig.	77.83	18.99	14.35	84.39	67.75	58.18
	Ours	78.46	55.74	49.13	82.25	61.24	52.18
ITODD	Orig.	18.40	21.10	15.00	51.10	50.40	44.00
	Ours	28.70	23.50	13.90	54.00	52.40	44.80

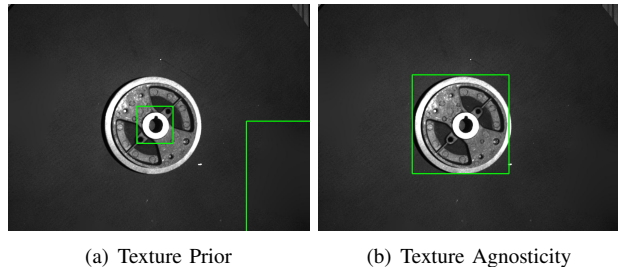


Fig. 4. **Detection example.** Example image from the ITODD test set, with bounding boxes predicted by the texture prior YOLOx and the texture agnostic variant; detection and IoU thresholds are both set to 0.5.

Superposition of online data augmentation and texture agnosticity for object detection.

The right part of Figure 5 shows the detection accuracy of Faster R-CNN on the TLESS dataset using our simple strategy for scaling online data augmentation with the coefficient λ , as presented in Section IV-B. Using this simple strategy for scaling augmentations proves to be sufficient to achieve comparable results to the baseline when using a λ value in the range of $0.2 \leq \lambda \leq 0.4$. The results in Figure 4 further indicate that texture agnosticity has a similar effect as online data augmentation on the learned representations and that careful tuning of the superposition of both might improve over simply using online data augmentations.

In summary, the main findings suggest that randomized texturing enhances performance for textureless and metallic objects, particularly when no online data augmentation method is applied. Training with a combination of randomly textured

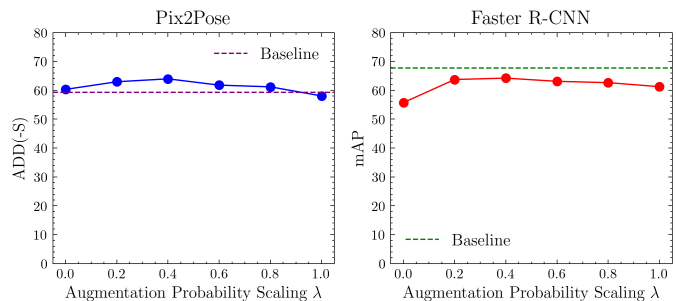


Fig. 5. **Online data augmentation severity.** Ablation study on the severity of online augmentation, for Pix2Pose and Faster R-CNN on TLESS; average recall of ADD(-S) score is reported; ground truth detections for pose estimation.

TABLE IV

POSE ESTIMATION PERFORMANCE. GDR-NET AND PIX2POSE TRAINED WITH ORIGINAL TEXTURES (BASELINE) AND RANDOMLY SELECTED TEXTURES APPLIED TO TLESS AND ITODD; ONE POSE ESTIMATION MODEL TRAINED PER OBJECT; YOLOX DETECTION RESULTS FROM BOP 2022 USED FOR POSE ESTIMATION

Dataset		GDR-Net				Pix2Pose			
		AR _{MSPD}	AR _{MSSD}	AR _{VSD}	AR	AR _{MSPD}	AR _{MSSD}	AR _{VSD}	AR
TLESS	Original	65.04	46.36	42.04	51.15	72.41	40.77	36.69	49.96
	Random (ours)	68.59	50.61	45.93	55.03	76.25	43.23	38.46	52.65
ITODD	Original	14.30	10.00	7.80	10.70	28.90	11.70	10.80	17.20
	Random (ours)	15.30	10.20	7.90	11.10	26.70	11.60	12.40	16.90

objects and online data augmentation consistently improves object detection performance for metallic objects, yet requires hyperparameter tuning of the applied online data augmentation to result in state-of-the-art performance.

2) *Pose Estimation Accuracy:* Object pose estimation is evaluated with GDR-Net [34] and Pix2Pose [25]. Besides the RGB image, both methods require sparse location priors in image space as input. We use the detections generated by YOLOx, provided by the winning method of the 2022 BOP [22], as location priors [7].

Table IV compares GDR-Net and Pix2Pose trained with texture priors and agnosticity. Texture agnosticity improves pose estimation recall of GDR-Net for TLESS by 3.88% and ITODD by 0.4%. The individual metrics AR_{MSPD}, AR_{MSSD}, and AR_{VSD} show similar increases on TLESS for both methods, indicating that randomized texturing improves equally across all aspects of pose estimation. The 3.53% increase in AR_{VSD}, which considers only visible pixels, indicates increased accuracy in occluded scenes. Selected samples from the TLESS dataset with estimated 3D bounding boxes are shown in Figure 6.

On ITODD, both methods generally struggle to achieve high accuracy on the standard pose estimation metrics used for evaluation. This limited performance results from the challenging object materials, i.e. metal, and the camera viewpoints in the test set, which only provide top-view captures of the objects. While GDR-Net shows improved performance, Pix2Pose shows marginally worse. Yet, our experiments indicate that our texture-agnostic variant, which only requires the object

geometry as input during training time, results in similar or improved results for metallic objects.

Superposition of online data augmentation and texture agnosticity for object pose estimation. The left part of Figure 5 evaluates the relationship between online data augmentation and texture agnosticity for pose estimation. It shows similar behavior as for object detection. Again, using the simple scaling parameter introduced in Section IV-B shows that a λ value in the range of $0.2 \leq \lambda \leq 0.4$ leads to the most accurate pose estimates with the average recall of ADD(-S) score as metric. This ablation shows that careful hyperparameter tuning of the applied online data augmentation leads to improved performance compared to only using data augmentation.

In summary, inducing texture agnosticity for object pose estimation improves the pose estimation accuracy for texture-less objects. For metallic objects, texture agnosticity improves when using GDR-Net and is similar to texture priors using Pix2Pose. Again, we show that careful hyperparameter tuning further improves pose estimation accuracy.

B. Ablations

In this section, we present the results of the ablation studies showing the influence of the number of random textures n , the robustness against image perturbations, and the influence of the object geometry prior.

1) *Number of Random Textures:* We ablate the number of textures used during dataset generation. Table V reports the results for object detection with YOLOx and pose estimation with GDR-Net. Table V shows that increasing the number of randomly chosen textures per object improves the AR score for pose estimation with GDR-Net and the mAP for object detection with YOLOx on TLESS. Ultimately, using

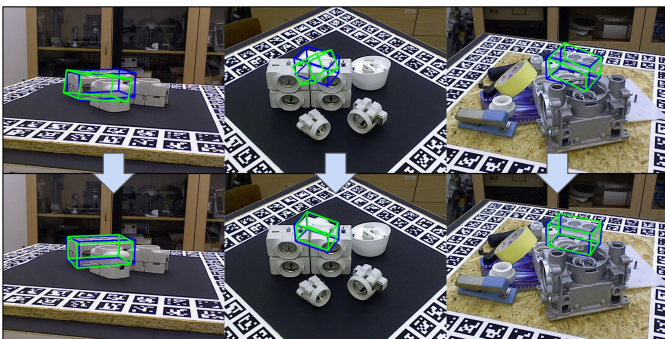


Fig. 6. **Pose estimation example.** Example images from the TLESS dataset, showcasing the increased performance for occluded object pose estimation; top row showing baseline estimations, bottom row the randomized texturing ones; GDR-Net for pose estimation and YOLOx for detection

TABLE V

NUMBER OF TEXTURES. ABLATION ON THE INFLUENCE OF THE NUMBER OF RANDOM TEXTURES, FOR YOLOX AND GDR-NET ON TLESS, USING AR; FOR POSE ESTIMATION ONE SHARED POSE ESTIMATION MODEL IS USED.

Number of Textures	YOLOx (mAP)	GDR-Net (AR)
$T_{n=3}$	65.57	31.25
$T_{n=5}$	72.38	33.01
$T_{n=7}$	73.53	35.75
$T_{n=1226}$	82.25	35.95

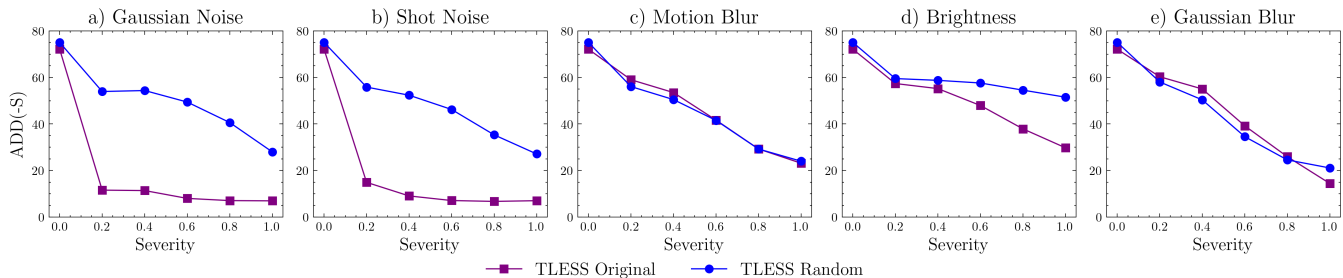


Fig. 7. **Robustness against image perturbations.** Influence of various image perturbations on ADD(-S) scores with varying severity; GDR-Net with one pose estimation model trained per object; ground truth detections used for pose estimation

$T_{n=1226}$ random textures, the maximum number of available cc-textures, yields the best performance in both cases.

2) *Robustness Against Image Perturbations:* To assess the robustness of texture priors and texture agnosticity against image perturbation, we report results on five common image perturbations [9]. The perturbations are applied to the test images of TLESS, using ground-truth detections as location priors for GDR-Net.

As shown in Figure 7, image perturbations influence the performance of GDR-Net differently when using texture priors or agnosticity. For the two noise-based perturbations (Subfigures a and b), texture agnosticity is consistently beneficial over different levels of severity. For the blur-based perturbations (Subfigures c and e), the performance loss of both variants is similar. Regarding brightness (refer to Subfigure d), texture agnosticity shows continuous resilience against increasing brightness changes, while the accuracy of the texture priors progressively worsens. In summary, randomized texturing increases overall robustness against image perturbations prominent in robotics applications.

3) *Influence of the Mesh Origin:* The TLESS dataset provides both CAD models and object reconstructions. Table VI ablates the influence of the mesh origin on the effectiveness of texture agnosticity. The AR for pose estimation is reported. Using reconstructions is generally inferior to using CAD models for training data generation. Inducing texture agnosticity with CAD models achieves the best performance. Conversely, rendering texture agnostic data from reconstructions is inferior to using the reconstructed texture. These findings showcase the usefulness of texture agnosticity despite not requiring texture information or color priors.

TABLE VI

MESH ORIGIN. POSE ESTIMATION ACCURACY USING PIX2POSE WITH DIVERSE COMBINATION OF OBJECT GEOMETRY AND TEXTURE, ON TLESS. THE GROUND TRUTH DETECTIONS AND AN AUGMENTATION PROBABILITY SCALING FACTOR OF $\lambda = 0.2$ ARE USED.

Mesh	Texture	AR
Reconstructed	Reconstructed	42.64
Reconstructed	Agnostic	46.57
CAD	Color Prior	59.24
CAD	Agnostic	62.95

VI. CONCLUSION

This paper presents a new approach for generating synthetic training data that encodes texture agnosticity to CNNs. We propose extending the domain randomization principle, which is easily applicable to state-of-the-art rendering pipelines. Our approach is especially beneficial when only object geometry priors without color or texture are available during training. We note that texture agnosticity is particularly useful for 6D object pose estimation. Object detection improves for metallic objects but struggles to improve results for textureless objects with some textural cues. For these cases, improving hyperparameters results in performance comparable to the baseline but not quite on par. Furthermore, we observe a significant increase in robustness toward image perturbations, which are relevant challenges of robotic vision applications.

Future studies will extend this work by adversarial texture generation, allowing models to learn the ideal texture distribution and investigate the influence of texture symmetries.

ACKNOWLEDGEMENT

We gratefully acknowledge the support of the EU-program EC Horizon 2020 for Research and Innovation under grant agreement No. 101017089, project TraceBot and the Austrian Science Fund (FWF), under project No. I 6114, project iChores.

REFERENCES

- [1] D. Bashkirova *et al.*, “VisDA-2021 competition: Universal domain adaptation to improve performance on out-of-distribution data,” in *NeurIPS 2021 Competitions and Demonstrations Track*. PMLR, 2022, pp. 66–79.
- [2] D. Bauer, T. Patten, and M. Vincze, “VeREFINE: Integrating object pose verification with physics-guided iterative refinement,” *IEEE Robotics and Automation Letters*, vol. 5, no. 3, pp. 4289–4296, 2020.
- [3] B. Calli, A. Walsman, A. Singh, S. Srinivasa, P. Abbeel, and A. M. Dollar, “Benchmarking in manipulation research: Using the Yale-CMU-Berkeley object and model set,” *IEEE Robotics & Automation Magazine*, vol. 22, no. 3, pp. 36–52, 2015.
- [4] M. Denninger *et al.*, “Blenderproc,” *CoRR*, vol. abs/1911.01911, 2019. [Online]. Available: <http://arxiv.org/abs/1911.01911>
- [5] B. Drost, M. Ulrich, P. Bergmann, P. Hartinger, and C. Steger, “Introducing MVTEC ITODD - A dataset for 3D object recognition in industry,” in *Proceedings of the IEEE International Conference on Computer Vision Workshops*, 2017, pp. 2200–2208.
- [6] L. A. Gatys, A. S. Ecker, and M. Bethge, “Image style transfer using convolutional neural networks,” in *Proceedings of the IEEE Conference on Computer Vision and Pattern Recognition*, 2016, pp. 2414–2423.
- [7] Z. Ge, S. Liu, F. Wang, Z. Li, and J. Sun, “YOLOX: Exceeding YOLO series in 2021,” *arXiv preprint arXiv:2107.08430*, 2021.

- [8] R. Geirhos, P. Rubisch, C. Michaelis, M. Bethge, F. A. Wichmann, and W. Brendel, "Imagenet-trained CNNs are biased towards texture; increasing shape bias improves accuracy and robustness." in *International Conference on Learning Representations*, 2019.
- [9] R. Geirhos, C. R. Temme, J. Rauber, H. H. Schütt, M. Bethge, and F. A. Wichmann, "Generalisation in humans and deep neural networks," *Advances in Neural Information Processing Systems*, vol. 31, 2018.
- [10] X. Glorot, A. Bordes, and Y. Bengio, "Domain adaptation for large-scale sentiment classification: A deep learning approach," in *Proceedings of the 28th International Conference on Machine Learning*, 2011, pp. 513–520.
- [11] K. He, G. Gkioxari, P. Dollár, and R. Girshick, "Mask R-CNN," in *Proceedings of the IEEE International Conference on Computer Vision*, 2017, pp. 2961–2969.
- [12] Z. He *et al.*, "ContourPose: Monocular 6-D pose estimation method for reflective textureless metal parts," *IEEE Transactions on Robotics*, vol. 39, no. 5, pp. 4037–4050, 2023.
- [13] Hinterstoisser *et al.*, "Model based training, detection and pose estimation of texture-less 3D objects in heavily cluttered scenes," in *11th Asian Conference on Computer Vision*, 2012, pp. 548–562.
- [14] T. Hodaň *et al.*, "BOP: Benchmark for 6D object pose estimation," in *Proceedings of the European Conference on Computer Vision*, 2018, pp. 19–34.
- [15] —, "Photorealistic image synthesis for object instance detection," in *IEEE International Conference on Image Processing*. IEEE, 2019, pp. 66–70.
- [16] —, "BOP challenge 2020 on 6D object localization," *Proceedings of the European Conference on Computer Vision Workshops*, 2020.
- [17] T. Hodaň, P. Haluza, Š. Obdržálek, J. Matas, M. Lourakis, and X. Zabulis, "T-LESS: An RGB-D dataset for 6D pose estimation of textureless objects," in *IEEE Winter Conference on Applications of Computer Vision*, 2017, pp. 880–888.
- [18] T. Ikeda, S. Tanishige, A. Amma, M. Sudano, H. Audren, and K. Nishiwaki, "Sim2Real instance-level style transfer for 6D pose estimation," in *IEEE International Conference on Intelligent Robots and Systems*, 2022, pp. 3225–3232.
- [19] D. Li, Y. Yang, Y.-Z. Song, and T. M. Hospedales, "Deeper, broader and artier domain generalization," in *Proceedings of the IEEE International Conference on Computer Vision*, 2017, pp. 5542–5550.
- [20] T.-Y. Lin *et al.*, "Microsoft COCO: Common objects in context," in *Proceedings of the European Conference on Computer Vision*, 2014, pp. 740–755.
- [21] T.-Y. Lin, P. Goyal, R. Girshick, K. He, and P. Dollár, "Focal loss for dense object detection," in *Proceedings of the IEEE International Conference on Computer Vision*, 2017, pp. 2980–2988.
- [22] X. Liu, R. Zhang, C. Zhang, B. Fu, J. Tang, X. Liang, J. Tang, X. Cheng, Y. Zhang, G. Wang, and X. Ji, "Gdrnpp," https://github.com/shanice-l/gdrnpp_bop2022, 2022.
- [23] P. Martinez-Gonzalez, S. Oprea, A. Garcia-Garcia, A. Jover-Alvarez, S. Orts-Escolano, and J. Garcia-Rodriguez, "UnrealROX: An extremely photorealistic virtual reality environment for robotics simulations and synthetic data generation," *Virtual Reality*, 2019.
- [24] B. Mildenhall, P. P. Srinivasan, M. Tancik, J. T. Barron, R. Ramamoorthi, and R. Ng, "NeRF: Representing scenes as neural radiance fields for view synthesis," *Communications of the ACM*, vol. 65, no. 1, pp. 99–106, 2021.
- [25] K. Park, T. Patten, and M. Vincze, "Pix2Pose: Pixel-wise coordinate regression of objects for 6D pose estimation," in *Proceedings of the IEEE/CVF International Conference on Computer Vision*, Oct 2019.
- [26] S. Ren, K. He, R. Girshick, and J. Sun, "Faster R-CNN: Towards real-time object detection with region proposal networks," *Advances in Neural Information Processing Systems*, vol. 28, 2015.
- [27] O. Russakovsky, J. Deng, H. Su, J. Krause, S. Satheesh, S. Ma, Z. Huang, A. Karpathy, A. Khosla, M. Bernstein, A. C. Berg, and L. Fei-Fei, "ImageNet Large Scale Visual Recognition Challenge," *International Journal of Computer Vision (IJCV)*, vol. 115, no. 3, pp. 211–252, 2015.
- [28] M. Suchi, B. Neuberger, A. Salykov, J.-B. Weibel, T. Patten, and M. Vincze, "3d-dat: 3d-dataset annotation toolkit for robotic vision," in *2023 IEEE International Conference on Robotics and Automation (ICRA)*, 2023, pp. 9162–9168.
- [29] Y. Sun, J. Falco, M. A. Roa, and B. Calli, "Research challenges and progress in robotic grasping and manipulation competitions," *IEEE Robotics and Automation Letters*, vol. 7, no. 2, pp. 874–881, 2022.
- [30] M. Sundermeyer *et al.*, "Bop challenge 2022 on detection, segmentation and pose estimation of specific rigid objects," *Proceedings of the IEEE/CVF Conference on Computer Vision and Pattern Recognition*, 2023.
- [31] S. Thalhammer, M. Leitner, T. Patten, and M. Vincze, "PyraPose: Feature pyramids for fast and accurate object pose estimation under domain shift," in *IEEE International Conference on Robotics and Automation*, 2021, pp. 13 909–13 915.
- [32] S. Thalhammer, T. Patten, and M. Vincze, "COPE: End-to-end trainable constant runtime object pose estimation," in *Proceedings of the IEEE/CVF Winter Conference on Applications of Computer Vision*, 2023, pp. 2859–2869.
- [33] J. Tobin, R. Fong, A. Ray, J. Schneider, W. Zaremba, and P. Abbeel, "Domain randomization for transferring deep neural networks from simulation to the real world," in *IEEE/RSJ International Conference on Intelligent Robots and Systems*, 2017, pp. 23–30.
- [34] G. Wang, F. Manhardt, F. Tombari, and X. Ji, "GDR-Net: Geometry-guided direct regression network for monocular 6D object pose estimation," in *Proceedings of the IEEE/CVF Conference on Computer Vision and Pattern Recognition*, 2021, pp. 16 611–16 621.
- [35] J. Yang, W. Xue, S. Ghavidel, and S. L. Waslander, "6D pose estimation for textureless objects on RGB frames using multi-view optimization," in *IEEE International Conference on Robotics and Automation*, 2023, pp. 2905–2912.
- [36] L. Yang, Q. Yan, Y. Fu, and C. Xiao, "Surface reconstruction via fusing sparse-sequence of depth images," *IEEE Transactions on Visualization and Computer Graphics*, vol. 24, no. 2, pp. 1190–1203, 2018.